Modelling topical photodynamic therapy treatment including the continuous production of Protoporphyrin IX

Campbell, C. L.; Brown, C. T A; Wood, K.; Moseley, H.

Published in:
Physics in Medicine and Biology

DOI:
10.1088/0031-9155/61/21/7507

Publication date:
2016

Document Version
Peer reviewed version

Modelling topical photodynamic therapy treatment including the continuous production of Protoporphyrin IX

C L Campbell[1], C T A Brown[1], K Wood[1] and H Moseley[2]

[1] School of Physics and Astronomy, University of St Andrews, UK
[2] Photobiology Unit, Ninewells Hospital and Medical School, University of Dundee, UK

E-mail: clc57@st-andrews.ac.uk

April 2016

Abstract.

Most existing theoretical models of photodynamic therapy (PDT) assume a uniform initial distribution of the photosensitive molecule, Protoporphyrin IX (PpIX). This is an adequate assumption when the prodrug is systematically administered; however for topical PDT this is no longer a valid assumption. Topical application and subsequent diffusion of the prodrug results in an inhomogeneous distribution of PpIX, especially after short incubation times, prior to light illumination. In this work a theoretical simulation of PDT where the PpIX distribution depends on the incubation time and the treatment modality is described. Three steps of the PpIX production are considered. The first is the distribution of the topically applied prodrug, the second in the conversion from the prodrug to PpIX and the third is the light distribution which affects the PpIX distribution through photobleaching. The light distribution is modelled using a Monte Carlo radiation transfer model and indicates treatment depths of around 2 mm during daylight PDT and approximately 3 mm during conventional PDT. The results suggest that treatment depths are not only limited by the light penetration but also by the PpIX distribution.

1. Introduction

Photodynamic therapy (PDT) is a non-invasive light based therapy used for treating superficial skin lesions such as Aktinic Keratosis (AK) and Basal Cell Carcinoma (BCC). The combination of light, a photosensitive molecule and oxygen results in selective tissue destruction through the production of singlet oxygen (Wilson and Patterson, 2008). The photosensitive molecule Protoporphyrin IX (PpIX) is produced as a result of a topically applied prodrug, which diffuses into the skin. For topically applied PDT it is common to use precursors to the photosensitive molecule Porotporphyrin IX (PpIX) such as the naturally occurring amino acid 5-Aminolevulinenic acid (ALA)

or its methyl ester methyl aminolevulinate (MAL). The distribution of this prodrug and thereby the concentration of PpIX will depend on the distance from the surface and the total time since application. For topical PDT it is therefore important to include this inhomogeneous distribution (in the vertical plane) of the photosensitiser (Svaasand et al., 1996; van den Akker et al., 2000). This results in a more accurate dosimetry model compared to when the initial distribution of PpIX is assumed to be uniform (Campbell et al., 2015).

When choosing an appropriate light source for PDT there are several aspects to consider. Firstly, the wavelengths have to match the absorption bands of the photosensitiser so that a sufficient amount of singlet oxygen is produced. The illumination area has to be sufficient to treat the selected region and the irradiation has to be high enough to provide a good treatment response, whereas the irradiance has to be low enough to reduce the experienced pain. A typical light source used for conventional PDT is the Akilite (Photocure ASA, Hoffsveien, N-0377 Oslo, Norway) which is a red LED based light source (Moseley, 2005). This treatment modality is typically associated with pain during light illumination (Castano et al., 2004). An alternative treatment modality is daylight PDT, where daylight is used as the alternative therapeutic light source. This has been shown to result in a high response rate, a reduced experienced pain and the preferred choice of treatment from the patient's point of view (Wiegell et al., 2008, 2012, 2013, 2011). In the work presented here both conventional PDT as well as daylight PDT are considered.

During conventional PDT, the prodrug (containing either ALA or MAL) is topically administered to the lesion 3 hours before the light illumination. During this occlusive treatment phase, the prodrug diffuses through the skin and is subsequently converted within the mitochondria of the tumour cells to the photosensitive chemical PpIX (Wachowska et al., 2011; Donnelly et al., 2007; Aalders et al., 2001; Donnelly et al., 2005). For daylight PDT however this occlusive treatment phase is typically (only) 30 minutes (Morton et al., 2015).

To our knowledge there have been no theoretical investigations of PDT which takes into consideration these different treatment modalities. This paper introduces a Monte Carlo radiation transfer (MCRT) model of PDT where the temporal and spatial dependence of the PpIX production is considered. Previous studies have considered topical application of the prodrug to theoretically determine the distribution of the PpIX after the occlusive treatment phase. These different studies have used slightly different approaches (Svaasand et al., 1996; Star et al., 2002; Salas-García et al., 2012; Salas-García et al., 2014). The study by Star et al included the most complicated conversion model between the prodrug and the PpIX, however a maximum penetration depth of 0.5 mm was assumed. This contradicts other studies where a deeper penetration is indicated (Casas et al., 2000; Donnelly et al., 2007; Malik et al., 1995; Juzenas et al., 2009; Naghavi et al., 2011).

By combining both the PpIX production model with the MCRT model both light penetration limitations and drug penetration limitations can be explored. This results

in more appropriate representation of PDT for the different treatment conditions. The developed model invites discussion regarding the appropriateness of the length of the occlusive treatment phases and the effect of prolonged daylight exposure.

2. Methods

The production of PpIX as a result of topical administration of a prodrug is a complex procedure with multiple steps. The model presented here contains what is believed to be the most relevant parameters, thus reducing the number of required assumptions and approximations. The model is primarily based on basic molecular diffusion theory in combination with a simple rate equation. A one dimensional case was considered where the concentration of PpIX was assumed to only vary in the vertical direction (from the surface of the tissue). Firstly, the MCRT model will be described followed by an explanation of the PpIX production model.

2.1. Monte Carlo radiation transfer modelling

MCRT modelling is a numerical technique which utilises the probabilistic nature of the photon interactions to simulate the transport, scattering and absorption of light within scattering media. By tracking photons through their random walk, important information about the energy deposition and light distribution within the simulation volume during illumination can be generated. The code that was used throughout this work was developed from a publicly available FORTRAN code (Wood, 2013; Wood and R. J. Reynolds, 1999) which was originally developed for astronomy applications. The code has subsequently been adapted for simulating PDT and has been extensively validated (Campbell et al., 2015; Valentine et al., 2011).

The code simulates the propagation of photons through a three dimensional (3D) Cartesian grid containing 10^6 voxels. The dimensions of the simulation region were $10\,\mathrm{mm} \times 10\,\mathrm{mm} \times 10\,\mathrm{mm}$ and a cylindrical tumour region was placed in the centre of the grid with a diameter of 6 mm and a depth of 10 mm. The simulated photons were given an initial direction and wavelength and were launched from the surface of the grid such that the surface was evenly illuminated. The photons were subsequently tracked until they were either absorbed of scattered out of the simulation region. Repeated boundary conditions were adopted to simulate a semi-infinite tissue slab.

The scattering and absorption events are determined by the optical properties within each individual voxel. When a photon reaches an interaction location, the probability of the photon being scattered is determined by the albedo which is defined as,

$$a = \frac{\mu_s(\lambda)}{\mu_s(\lambda) + \mu_a(\lambda)} \tag{1}$$

where $\mu_\mathrm{s}(\lambda)$ and $\mu_\mathrm{a}(\lambda)$ corresponds to the wavelength dependent scattering and absorption coefficients associated with the skin tissue. The optical properties of the

skin tissue adopted in this work are the same as those used in previous work (Campbell et al., 2015; Yudovsky and Pilon, 2011; Salomatina et al., 2006). When adding a non-uniform distribution of PpIX, the optical absorption properties associated with the PpIX will also be non-uniform and vary with PpIX concentration. The absorption coefficient for PpIX will depend on the local number density of PpIX molecule such that,

$$\mu_{aPpIX}(\lambda) = n_{PpIX}\sigma_{PpIX}(\lambda) \tag{2}$$

where n_{PpIX} is the number density of PpIX molecules (cm^{-3}) and $\sigma_{PpIX}(\lambda)$ is the wavelength dependent PpIX cross section (cm^2) shown in figure 1.

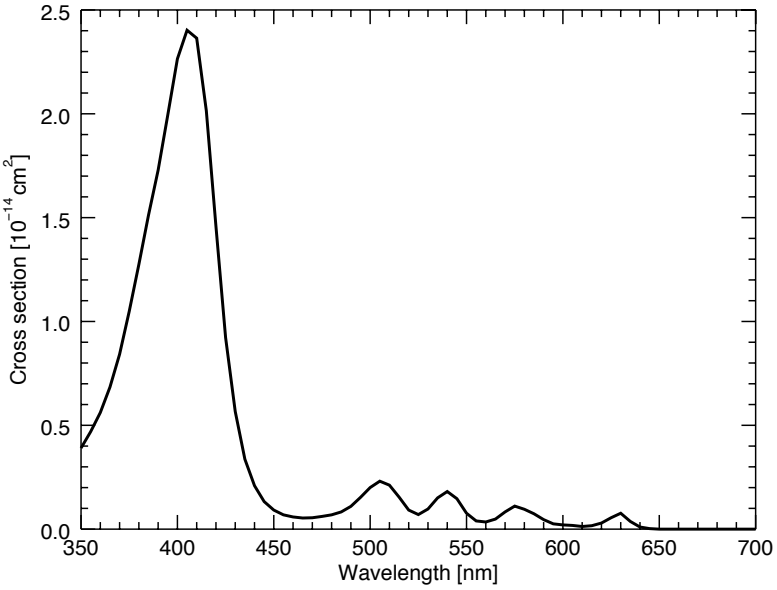

Figure 1: PpIX cross section as a function of wavelength. The absorption coefficient is generated by multiplying the cross section (displayed in the figure) with the PpIX number density of PpIX molecules present in each voxel (Salas-García et al., 2012).

If the photon is scattered as a result of an interaction event the new angular scattering direction is determined by the Henyey-Greenstein phase function (HG(θ)) (Henyey and Greenstein, 1941).

$$HG(\theta) = \frac{1}{4\pi}\frac{1-g^2}{(1+g^2-2gcos\theta)^{3/2}} \tag{3}$$

where θ is the scattering angle and g is the anisotropy factor which describes the nature of the scattering. g can take values in the range $-1 \leq$ g ≤ 1, where g $=$ 0 corresponds to isotropic scattering. In skin tissue, the scattering is predominantly forward scattering (g > 0). In the work presented here the wavelength dependent anisotropy factor $g(\lambda) = 0.62 + 0.29 \times 10^{-3}\lambda$ (with λ in nm) was adopted (Van Gemert

et al., 1989). The refractive index was assumed to be uinform throughout the skin tissue (n = 1.38) and Fresnel equations were adopted to determine the reflectance and refraction at the air/tissue interface.

2.2. Prodrug diffusion

The first step is to consider the diffusion of the prodrug since this dictates the distribution of PpIX molecules. Molecular diffusion, where molecules diffuse from a region of high concentration to a region of lower concentration is described by Fick's first law,

$$J = -D\frac{\partial M(z,t)}{\partial z} \tag{4}$$

where J corresponds to the flux vector which describes the flow of substance (molecules) through a unit area per unit time ($m^{-2}s^{-1}$). The magnitude of J is proportional to the gradient of the concentration M(z,t) (m^{-3}). In this case, M(z,t) corresponds to the number density of MAL molecules. D ($m^2\,s^{-1}$) is the diffusivity, or diffusion coefficient, which describes the speed at which a substance diffuses through another substance.

By applying the continuity equation for mass conservation (Svaasand et al., 1996),

$$\frac{\partial J}{\partial z} + \frac{\partial M(z,t)}{\partial t} = 0 \tag{5}$$

and combining with equation 4, the equation that describes how M(z,t) changes with time is,

$$\frac{\partial M(z,t)}{\partial t} = D\frac{\partial^2 M(z,t)}{\partial z^2} \tag{6}$$

By assuming that the initial concentration, M_0 is introduced at t=0 and z=0, and thereafter kept constant at M_0 the following solution satisfies equation 6 (Crank, 1975):

$$M(z,t) = M_0(1 - erf\left(\frac{z}{\sqrt{4Dt}}\right)) \tag{7}$$

where the gaussian error function (erf) is defined as

$$erf(u) = \frac{2}{\sqrt{\pi}}\int_0^u e^{-t^2}dt \tag{8}$$

This boundary condition was assumed due to the excess cream still present on the lesion after 3 hours of occlusive treatment, acting as a reservoir and thus the concentration of MAL (or ALA) molecules could be kept constant at the surface. Since the diffusion problem described here can be compared to a plane source with an extended initial distribution, the standard solution (equation 7) was believed to be an appropriate description of the prodrug diffusion. Similar assumptions have previously been argued for and applied in other studies where similar models were developed such as (Crank, 1975; Star et al., 2002; Svaasand et al., 1996; Salas-García et al., 2012; Salas-García

et al., 2014). A diffusion barrier is not considered in the presented model since these properties are to our knowledge not well characterised. It is believed that the diffusion barrier in a tumour region is reduced compared to healthy skin (Svaasand et al., 1996). In combination with a light curettage of the surface of the skin it is assumed, for the purpose of this study, that the diffusion barrier does not affect the diffusion of the cream. A reduced concentration of the prodrug at the upper part of the skin compared to previous studies is however assumed. We acknowledge that this is an initial first order approximation and that the concentration of prodrug at the upper part of the skin will only reach its maximum value after some time. However, we believe that for the purpose of this paper this assumption is sufficient. Future work should investigate the diffusion barrier of skin further.

2.3. PpIX production

PpIX is produced from ALA molecules. In the work presented here a prodrug containing MAL molecules was considered, however the conversion from MAL to ALA was not separately included and only the conversion from MAL to PpIX was considered in the equation describing the production of PpIX. The rate equation is expressed as follows (Svaasand et al., 1996; Star et al., 2002),

$$\frac{\partial P(z,t)}{\partial t} = -\frac{P(z,t)}{\tau_p} + \varepsilon_p \frac{M(z,t)}{\tau_{ap}} \tag{9}$$

Equation 9 includes the two main features that contribute to the resulting concentration of PpIX. The source term in the equation (term furthest to the right) corresponds to the conversion from MAL molecules to PpIX molecules. This depends on the distribution of MAL molecules, M(z,t), the yield, ε_{p}, which determines the proportion of MAL molecules being converted to PpIX, as well as the relaxation time, τ_{ap}. The relaxation time, τ_{ap} determines how fast this conversion happens and is defined as the time it takes for the concentration (M(z,t)) to reduce to 1/e (37 %) of its original concentration due to PpIX production. The sink in this equation is the first term to the right of the equal sign. This term corresponds to the clearance of the PpIX (mostly due to heme production). The rate at which the clearance mechanism happens is dictated by the relaxation time, τ_{p}.

The solution to equation 9 is (Svaasand et al., 1996) to be ,

$$P(z,t) = \frac{\varepsilon_p}{\tau_{ap}} \int_0^t e^{-\frac{t-t'}{\tau_p}} M(z,t')dt' = \frac{M_0 \varepsilon_p}{\tau_{ap}} \int_0^t e^{-\frac{t-t'}{\tau_p}} (1 - erf\left(\frac{z}{\sqrt{4Dt'}}\right))dt' \tag{10}$$

To establish the resulting PpIX concentration due to the PpIX production model, the parameters M_0, ε_{p}, τ_{ap}, τ_{p} and D have to be established. The parameters used for the work presented here were taken from the literature and are summarised in table 1. The initial cream concentration M_0 was chosen such that it lies between two extremes. In previous publications the initial uniform concentration of PpIX has been assumed to be around $10^{14}\,\mathrm{cm}^{-3}$ (Campbell et al., 2015), while work by Salas Garcia et al has suggested

an initial concentration of MAL molecules to be around $10^{20}\,\mathrm{cm}^{-3}$ (Salas-García et al., 2012). For this reason a value of 6×10^{16} MAL molecules per cubic centimetre was chosen for the present study. Even though the concentration of the cream has been reported to be of the orders of $10^{20}\,\mathrm{cm}^{-3}$ it is assumed that a diffusion barrier reduced the amount of cream passing through it. Hence it is assumed that $6 \times 10^{16}\,\mathrm{cm}^{-3}$ is the concentration of MAL molecules in the top layer of the skin.

Table 1: Parameters used to determine the PpIX production

Parameter	value	
M_0 [cm^{-3}]	6×10^{16}	
ε_p	0.5	(Salas-García et al., 2012)
τ_ap [s]	8640	(Star et al., 2002)
τ_p [s]	4680	(Star et al., 2002)
D [$\mathrm{m}^2\,\mathrm{s}^{-1}$]	0.69×10^{-10}	(Salas-García et al., 2012; Svaasand et al., 1996)

2.4. Photobleaching

The equation described above does not include any light interaction and only considers the production of PpIX. When PpIX interacts with light, the concentration of PpIX molecules reduces with time due to photobleaching. This type of reduction of concentration was considered within the MCRT model but was however not included in the rate equation (equation 9). Therefore it was assumed that the concentration reduction due to photobleaching did not affect the diffusion of the prodrug molecules or the production of PpIX. The photobleaching is assumed to only depend on the fluence rate as well as the initial PpIX concentration (Jacques et al., 1993; Farrell et al., 1998; Robinson et al., 1998; Valentine et al., 2011; Jongen and Sterenborg, 1997). The photobleaching adopted in the work here was expressed using the following equation,

$$C(x, y, z, t) = C_0(x, y, z)e^{-\psi(x,y,z)t/\beta(\lambda)} \tag{11}$$

where $\mathrm{C(x, y, z, t)}$ is the local time dependent PpIX concentration, $\mathrm{C_0(x, y, z)}$ corresponds to the distribution of PpIX which depends on equation 10 as well as the different treatment modalities (see section 2.5). $\psi(\mathrm{x, y, z})$ is the local fluence rate in $\mathrm{W\,cm}^{-2}$ which is computed within the MCRT model. The wavelengths dependent photobleaching dose constant, $\beta(\lambda)$ is defined as,

$$\beta(\lambda) = \beta(630)\frac{\mu_{aPpIX}(630)}{\mu_{aPpIX}(\lambda)}\frac{630}{\lambda} \tag{12}$$

Here $\mu_{\mathrm{aPpIX}}(630)$ is the absorption coefficient of PpIX at 630 nm and $\beta(630)$ is the photobleaching constant at 630 nm which has previously been determined to be 14 $\mathrm{J\,cm}^{-2}$ (Valentine et al., 2011). λ is the wavelength (in nm) of the simulated photon and μ_{aPpIX} is the absorption coefficient of PpIX at that wavelength. The photobleaching

was considered within the MCRT code by introducing an iterative time dynamic where 5×10^6 photons were launched during each time step. At the end of each time step the PpIX concentration was updated prior to launching a new set of photons. This number of photons (5×10^6) was implemented to ensure that a good signal to noise ratio was achieved within a reasonable simulation time. The number of time steps varied depending on the light condition that was simulated since these corresponded to different simulated treatment times. Since the majority of the interaction occurs at the start of the treatment, the time steps were assumed to be shorter at the start of the simulated treatment.

2.5. Different treatment modalities

During the occlusive treatment phase of conventional PDT the region of interest is covered with an occlusive dressing. Before the light irradiation the dressing, and any excess cream, is removed from the lesion. When daylight is used as the alternative light source there is no occlusive dressing applied and any excess cream is left on the lesion for the duration of the treatment. Since the amount of exposure will be different for different patients during daylight PDT, for the work presented here it was assumed that the occlusive treatment phase during daylight PDT was similar to conventional PDT.

The differences between the two treatment modalities that are simulated are summarised in table 2. The most important difference is the continued accumulation and production of PpIX during the light treatment for daylight PDT. While the production of PpIX is assumed to be interrupted as the cream is removed prior to illumination during conventional PDT. This is motivated by the short illumination time (15 minutes) relative to the long occlusion (3 hours). These differences have to be considered when determining the photobleaching discussed above. For each time iteration the initial concentration in equation 11 has to be updated during daylight PDT since the PpIX is assumed to continue to be produced. For this reason the concentration reduction due to photobleaching as well as the concentration increase due to PpIX production have to be considered during each time iteration.

Table 2: Description of the different treatment modalities where the PpIX is assumed to continue to buildup during the light interaction phase of the treatment during daylight PDT but not during conventional PDT. These properties are based on established clinical practice (Morton et al., 2015).

Concept	Conventional PDT	Daylight PDT
Occlusive treatment, no light	3 hours	30 minutes
PpIX build up during illumination	NO	YES
Photobleaching during illumination	YES	YES

2.6. Light sources

In the MCRT model, the incident wavelengths are sampled such that the probability distribution of the irradiance, and therefore the light spectra of the different light sources are reproduced. The light spectra used to simulate both conventional PDT and daylight PDT are shown in figure 2. The light source that is used to simulate conventional PDT is the Aktilite and the total irradiance for this light source was assumed to be 82 mW cm^{-2}. To simulate daylight PDT, both the direct and diffuse components are included since this allows for different weather conditions to be simulated. For daylight during clear conditions it was assumed that 80% of the total illumination was direct daylight while 20% was diffuse daylight with a total irradiance of 41 mW cm^{-2}. During overcast condition the total illumination was assumed to contain 100% diffuse daylight with a total irradiance of 8 mW$\dot{c}$m^{-2}.

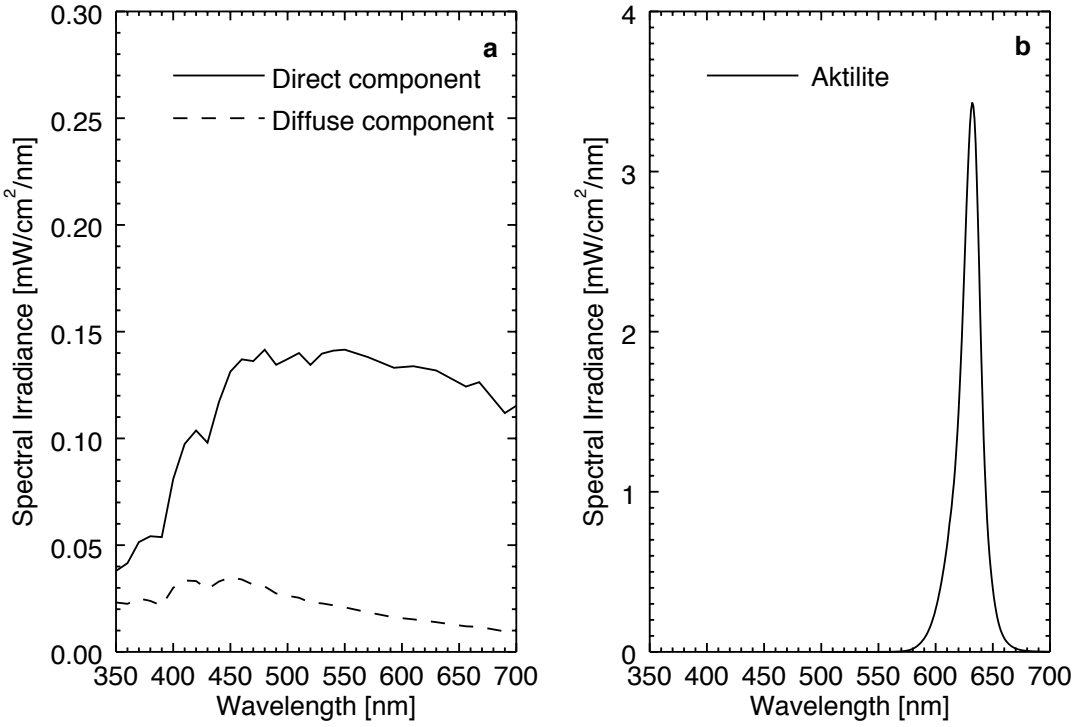

Figure 2: Figure showing the spectra included in the theoretical model. a) Light spectra of both the direct and diffuse component of Daylight (Bird and Riordan, 1986). b) Light spectrum of the Aktilite (Moseley, 2005), which is the typical light source simulated for conventional PDT.

These different light conditions were used to simulate different PDT treatment conditions. Our model was used to determine the photodynamic dose (PDD) for these different treatment conditions where the PDD is defined as the number of absorbed

photons, by the photosensitiser (PpIX), per unit volume (Farrell et al., 1998). Here we adopt a toxic threshold as an approximation of the number of required absorption events to achieve an effective treatment outcome. The value for the toxic threshold of 8.6×10^{17} photons cm^{-3} was adopted for illustrative purposes. This value has previously been determined from measurements of Photofrin in liver tissue (Patterson et al., 1990).

3. Results

To demonstrate the build up of PpIX during the occlusive treatment phase (excluding any light interaction) figure 3 shows the depth dependent concentration of PpIX after 30 min, 60 min and 180 min of occlusive treatment. The model successfully demonstrates the increase in PpIX concentration with depth for prolonged incubation time.

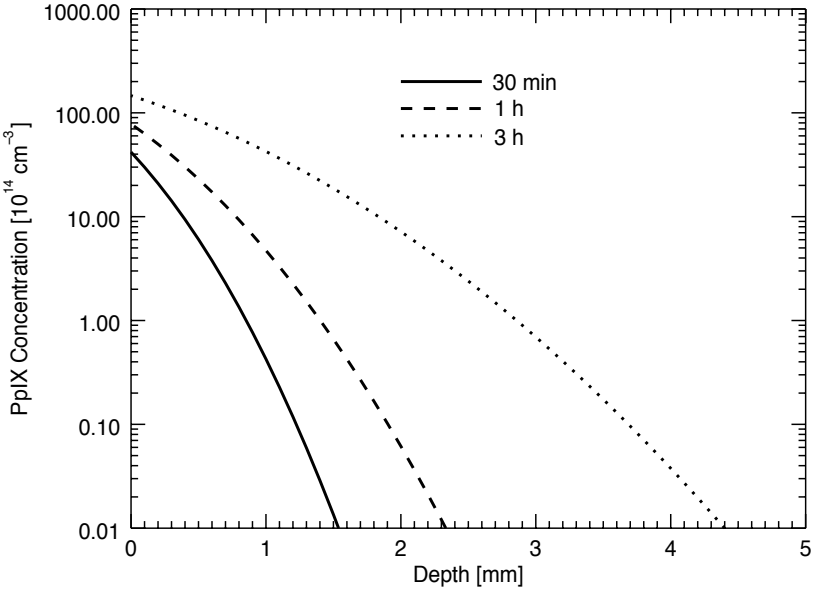

Figure 3: Figure showing the number density of PpIX molecules as a function of depth as it builds up with time. Three different incubation times (30 min (solid), 1 hour (dashed) and 3 hours (dotted)) are represented. This assumes no light interaction during the production of PpIX. The incubation times are measured from the time of drug application where an increased incubation time allows the concentration of PpIX molecules to build up for longer.

As previously mentioned during the light interaction phase of conventional PDT, it was assumed that there was no further production of PpIX. For this reason the concentration of PpIX was assumed to only be affected by the concentration reduction caused by photobleaching. However during daylight PDT the level of PpIX was not only reduced due to photobleaching but the PpIX was also assumed to continue to be

produced. The concentration of PpIX at different time points during illumination is demonstrated in figure 4. The different time points are represented by light dose, where the same light doses (10, 20, 40 and 75 $\mathrm{J\,cm^{-2}}$) are compared for the different light conditions. The light dose is defined as the irradiance of the light source multiplied by the total treatment time. Here the irradiance of daylight is defined over the wavelength range 350 - 700 nm. Both daylight during clear and overcast conditions are represented as well as the illumination by the Aktilite. For daylight PDT, PpIX is produced during the light treatment which generated a different reduction compared to the conventional PDT situation. Daylight PDT during overcast conditions resulted in overall larger concentrations of PpIX within the tumour tissue compared to treatment during clear conditions. This is due to the the prolonged treatment time required to deliver the total light dose of 75 $\mathrm{J\,cm^{-2}}$ during overcast conditions, allowing more PpIX molecules to be produced within the tumour tissue.

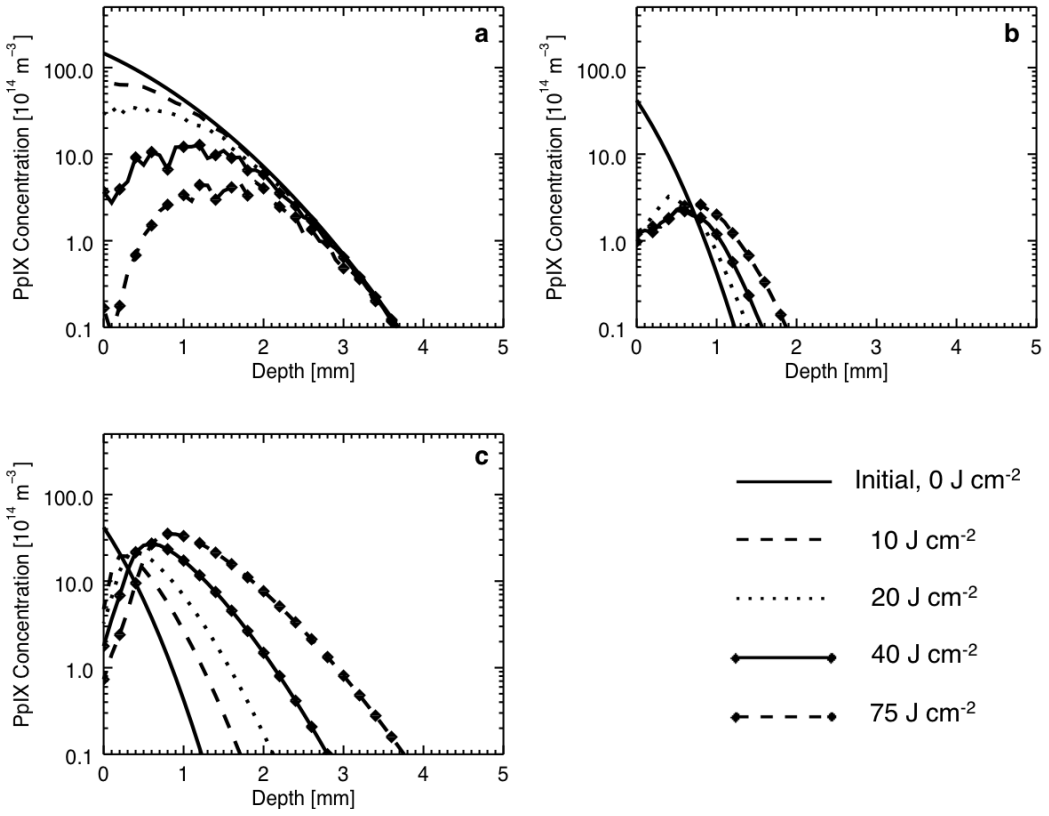

Figure 4: Representation of the change in the PpIX distribution during the light treatment. Three different light conditions were compared where a) demonstrates conventional PDT where the Aktilite was used as the illuminating light source assuming an occlusion of 3 hours and an irradiance of 82 $\mathrm{mW\,cm^{-2}}$, b) demonstrates daylight PDT during clear weather conditions (30 min of occlusion and irradiance of 41 $\mathrm{mW\,cm^{-2}}$) and c) demonstrates daylight PDT during overcast conditions (30 min of occlusion and irradiance of 8 $\mathrm{mW\,cm^{-2}}$).

Figure 5 demonstrates the photodynamic dose for the three different treatment conditions after a total delivered light dose corresponding to 75 J cm^{-2} (Valentine et al., 2011). The photodynamic dose is defined as the number of absorbed photons per cubic centimeter by the photosensitiser. This is a typical light dose delivered for conventional PDT treatments and is therefore the treatment light dose that is compared. The figure shows that the simulated treatment depth is not only dependent on the light penetration but also on the depth dependent production of PpIX.

For daylight PDT during clear conditions different incubation times were explored. Occlusive treatment phases of length 0 min, 30 min and 60 min were compared and the results are shown in figure 6. By allowing the PpIX to build up for a longer period of time prior to treatment, a deeper treatment is achieved.

4. Discussion

The different parameters associated with the PpIX production model such as the different relaxation times, diffusion coefficient and initial concentrates, are vital to accurately represent the distribution of PpIX within the tumour tissue. The values used for the relaxation times agree with studies published by Star et al and Aalders et al (Star et al., 2002; Aalders et al., 2001). Other studies suggest considerably different values for the relaxation time. Salas Garcia et al suggested that $\tau_{\mathrm{p}} = 84$ ms and $\tau_{\mathrm{ap}} = 24$ h (Salas-García et al., 2012; Salas-García et al., 2014). These can be argued to be unrealistic, especially since 84 ms is the non-radiative relaxation time of the PpIX molecule (Jiménez Pérez et al., 2008). Further studies are required to enable accurate determination of the parameters adopted in this model.

For the adopted parameters, the resulting achieved effective treatment depth for conventional PDT is comparable to those achieved when assuming an uniform initial distribution of PpIX (Campbell et al., 2015). The results presented here (under the stated assumptions) suggest that when simulating conventional PDT an uniform initial distribution of PpIX is not an unreasonable assumption for the conditions presented here. This will however strongly depend on the initial concentration and toxic threshold that is assumed. When simulating daylight PDT the work presented here suggests a larger dependence on the PpIX production. When assuming an initial uniform distribution of PpIX, clear weather conditions indicates a deeper simulated treatment compared to cloudy weather conditions. For the case presented here, assuming the same light dose, the cloudy conditions indicates a deeper simulated treatment compared to the clear conditions. This is explained by the prolonged treatment required during cloudy conditions to reach the light dose of 75 J cm^{-2}, which subsequently allows for additional PpIX production.

The sensitivity of the parameters in equation 10 were explored by increasing and decreasing their value in relation to the set of parameters adopted here. A reduced and increased value of $\frac{\varepsilon_0 \mathrm{M}_0}{\tau_{\mathrm{ap}}}$ results in a concentration profile of the PpIX that is scaled linearly. For an adjusted τ_{p}, the concentration profile is not scaled linearly due to the

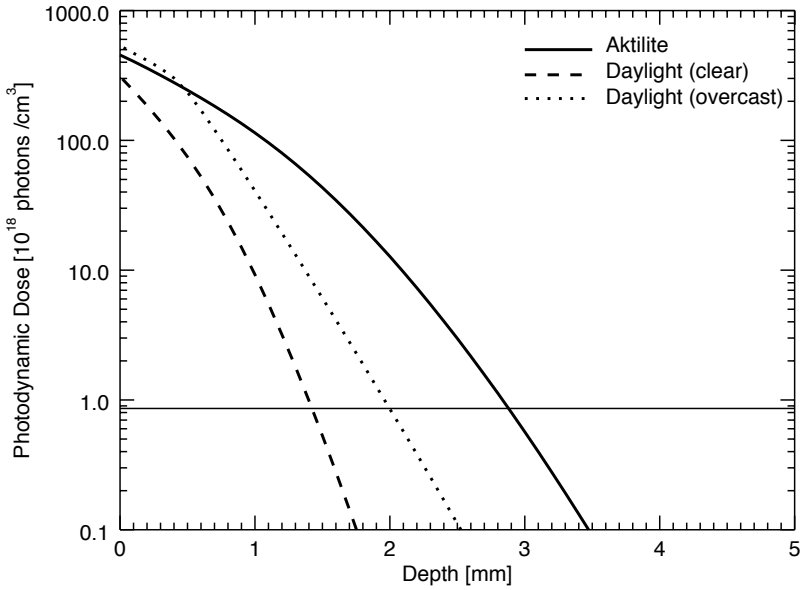

Figure 5: Photodynamic dose (PDD) as a function of depth for conventional PDT (Aktilie, solid) compared to daylight PDT during clear conditions (dashed) and overcast conditions (dotted). The PDD after a total delivered light dose of 75 $\mathrm{J\,cm^{-2}}$ is represented. The horizontal line corresponds to the toxic threshold which is an approximation of the number of photons required to be absorbed by the PpIX to achieve an effective treatment.

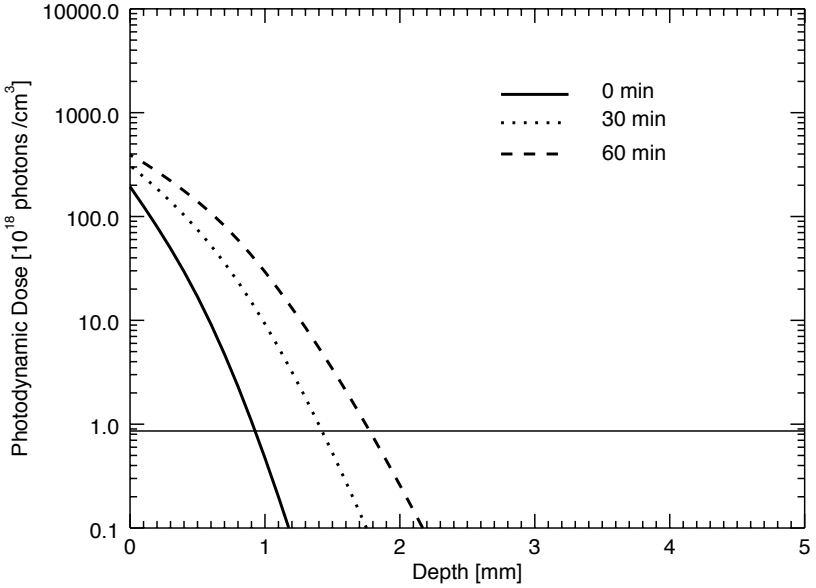

Figure 6: Photodynamic dose (PDD) as a function of depth for three different initial starting points after a total delivered light dose of 75 $\mathrm{J\,cm^{-2}}$ for daylight PDT (clear conditions). The occlusive treatment times of 0 min (solid), 30 min (dotted) and 60 min (dashed) are compared.The horizontal line corresponds to the toxic threshold.

nature of equation 10. Hence a reduced τ_p has a lager effect on the PpIX distribution and thereby the treatment depth compared to an increased tau_p. For example, if tau_p was reduced by a factor of 100, the resulting treatment depth (assuming the toxic threshold adopted here) would be reduced by approximately 0.5 mm. If tau_p was increased by the same factor however, the resulting treatment depth would not be greatly affected. A reduced diffusion coefficient results in slow and shallow distribution of PpIX and an increased diffusion coefficient results in a more uniform distribution of PpIX due to the faster diffusion of the prodrug. This consequently has the same effect on the effective treatment depth. Adjusted parameters results in different concentration profiles of PpIX which subsequently affects the effective treatment depth. Hence the treatment is not only limited by light penetration but is also strongly affected by the distribution and production of PpIX within the skin tissue.

The model presented here includes only the most important steps in the PpIX production dynamic however there are clearly other aspects that could be considered in future studies. These include the assumption that the PpIX did not diffuse from the location where it is produced. It was also assumed that the location of the PpIX within the cell did not change with time and thereby affect the treatment outcome. Additionally it was also assumed that the concentration gradient of MAL molecules was not affected by the production of PpIX or the photobleaching. It was also assumed that the light penetration was not affected by the presence of the cream on the surface of the lesion during daylight PDT. These, as well as the permeability of the cream through skin tissue, are aspects of the models that for future developments should be considered. The oxygen depletion during PDT was not considered and an unlimited oxygen supply was assumed. It can be argued that the oxygen depletion during treatment will result in a reduced production of PpIX. However, since the reduction of oxygen during PDT is poorly understood, we have chosen to assume an unlimited supply.

The results from the study suggest that if PpIX is being produced during the full daylight treatment, an extended treatment is to be recommended. A longer treatment, during lower light intensities will allow deeper situated PpIX and therefore a possible deeper treatment. However, when only considering superficial lesions (Fitzmaurice and Eisen, 2016), a shorter treatment and thereby a more superficial effective treatment could be sufficient for a successful result.

The diffusion model presented here is a major step forward towards a more accurate representation of different treatment modalities. By adopting reasonable values for the PpIX production parameters (C_0, ε_p, τ_{ap}, τ_p and D) the model indicates that the treatment depth is not only limited by the penetration of light but also by the drug diffusion and PpIX production rate. These are important factors to consider when calculating and optimising PDT dosimetry. Our results highlight that when considering daylight PDT is it important to consider these aspects of the treatment.

5. Conclusion

The incubation time associated with different treatment modalities results in different initial distributions of the photosensitive molecule PpIX. A non-uniform distribution of PpIX was investigated where a model was developed which depends on both the distance from the surface as well as the time passed since prodrug application. The results from the model suggest that treatment depths associated with PDT are not only limited by the penetration of the light but also by the penetration of the prodrug as well as the production of PpIX. Even though further investigation is required to establish the distribution parameters, the work presented here is a significant step towards more accurate theoretical predictions of PDT during different treatment conditions. Including a time dependent PpIX production model is key in driving the theoretical simulation of light based therapies forward.

Acknowledgments

C L Campbell acknowledges financial support from an UK EPSRC PhD studentship (EP/K503162/1) and the Alfred Stewart Trust.

References

Aalders, M. C. G., Van Der Vange, N., Star, W. M., and Sterenborg, H. J. C. M. (2001). A mathematical evaluation of dose-dependent ppix fluorescence kinetics in vivo. *Photochemistry and Photobiology*, 74(2):311–317.

Bird, R. and Riordan, C. (1986). Simple Solar Spectral Model for Direct and Diffuse Irradiance on Horizontal and Tilted Planes at the Earth's Surface for Cloudless Atmospheres. *Journal of Applied Meteorology*, 25:87–97.

Campbell, C., Wood, K., Valentine, R., Brown, C., and Moseley, H. (2015). Monte carlo modelling of daylight activated photodynamic therapy. *Physics in medicine and biology*, 60(10):4059.

Casas, A., Fukuda, H., Di Venosa, G., and Del C.batlle, A. (2000). The influence of the vehicle on the synthesis of porphyrins after topical application of 5-aminolaevulinic acid. implications in cutaneous photodynamic sensitization. *British Journal of Dermatology*, 143(3):564–572.

Castano, A., Demidova, T., and Hamblin, M. (2004). Mechanisms in photodynamic therapy: part one - photosensitizers, photochemistry and cellular localization. *Photodiagnosis and Photodynamic Therapy*, 1(4):279 – 293.

Crank, J. (1975). *The mathematics of diffusion / by J. Crank*. Clarendon Press Oxford [England], 2nd ed. edition.

Donnelly, R. F., McCarron, P. A., and Woolfson, A. D. (2005). Drug delivery of aminolevulinic acid from topical formulations intended for photodynamic therapy. *Photochemistry and Photobiology*, 81(4):750–767.

Donnelly, R. F., McCarron, P. A., and Woolfson, A. D. (2007). Derivatives of 5-aminolevulinic acid for photodynamic therapy. *Perspectives in Medicinal Chemistry*, 1:49–63.

Farrell, T., Hawkes, R., Patterson, M., and Wilson, B. (1998). Modeling of photosensitizer fluorescence emission and photobleaching for photodynamic therapy dosimetry. *Appl. Opt.*, 37(31):7168–7183.

Fitzmaurice, S. and Eisen, D. B. (2016). Daylight photodynamic therapy: What is known and what is yet to be determined. *Dermatologic Surgery*, 42(3):286–295.

Henyey, L. and Greenstein, J. (1941). Diffuse radiation in the Galaxy. , 93:70–83.

Jacques, S., Joseph, R., and Gofstein, G. (1993). How photobleaching affects dosimetry and fluorescence monitoring of pdt in turbid media. *Proc. SPIE*, 1881:168–179.

Jiménez Pérez, J. L., Cruz-Orea, A., Ramn-Gallegos, E., Gutierrez Fuentes, R., and Sanchez Ramirez, J. F. (2008). Photoacoustic spectroscopy to determine in vitro the non radiative relaxation time of protoporphyrin ix solution containing gold metallic nanoparticles. *The European Physical Journal Special Topics*, 153(1):353–356.

Jongen, A. and Sterenborg, H. (1997). Mathematical description of photobleaching in

vivo describing the influence of tissue optics on measured fluorescence signals. *Physics in Medicine and Biology*, 42(9):1701.

Juzenas, P., Juzeniene, A., Iani, V., and Moan, J. (2009). Depth profile of protoporphyrin ix fluorescence in an amelanotic mouse melanoma model. *Photochemistry and Photobiology*, 85(3):760–764.

Malik, Z., Kostenich, G., Roitman, L., Ehrenberg, B., and Orenstein, A. (1995). Topical application of 5-aminolevulinic acid, {DMSO} and edta: protoporphyrin {IX} accumulation in skin and tumours of mice. *Journal of Photochemistry and Photobiology B: Biology*, 28(3):213 – 218.

Morton, C., Wulf, H., Szeimies, R., Gilaberte, Y., Basset-Seguin, N., Sotiriou, E., Piaserico, S., Hunger, R., Baharlou, S., Sidoroff, A., et al. (2015). Practical approach to the use of daylight photodynamic therapy with topical methyl aminolevulinate for actinic keratosis: a european consensus. *Journal of the European Academy of Dermatology and Venereology*.

Moseley, H. (2005). Light distribution and calibration of commercial pdt led arrays. *Photochem. Photobiol. Sci.*, 4:911–914.

Naghavi, N., Miranbaygi, M., and Sazgarnia, A. (2011). Simulation of fractionated and continuous irradiation in photodynamic therapy: study the differences between photobleaching and singlet oxygen dose deposition. *Australasian Physical Engineering Sciences in Medicine*, 34(2):203–211.

Patterson, M. S., Wilson, B., and Graff, R. (1990). In vivo tests of the concept of photodynamic threshold dose in normal rat liver photosensitized by aluminum chlorosulphonated phthalocyanine. *Photochemistry and Photobiology*, 51(3):343–349.

Robinson, D., de Bruijn, H., van der Veen, N., Stringer, M., Brown, S., and Star, W. (1998). Fluorescence photobleaching of ala-induced protoporphyrin ix during photodynamic therapy of normal hairless mouse skin: the effect of light dose and irradiance and the resulting biological effect. *Photochem Photobiol*, 67(1):140–9.

Salas-García, I., Fanjul-Vélez, F., and Arce-Diego, J. L. (2014). Superficial radially resolved fluorescence and 3d photochemical time-dependent model for photodynamic therapy. *Opt. Lett.*, 39(7):1845–1848.

Salas-García, I., Fanjul-Vlez, F., and Arce-Diego, J. L. (2012). Photosensitizer absorption coefficient modeling and necrosis prediction during photodynamic therapy. *Journal of Photochemistry and Photobiology B: Biology*, 114(0):79 – 86.

Salomatina, E., Jiang, B., Novak, J., and Yaroslavsky, A. N. (2006). Optical properties of normal and cancerous human skin in the visible and near-infrared spectral range. *Journal of Biomedical Optics*, 11(6):064026–064026–9.

Star, W. M., Aalders, M. C. G., Sac, A., and Sterenborg, H. J. C. M. (2002). Quantitative model calculation of the time-dependent protoporphyrin ix concentration in normal human epidermis after delivery of ala by passive topical application or iontophoresis. *Photochemistry and Photobiology*, 75(4):424–432.

Svaasand, L. O., Wyss, P., Wyss, M.-T., Tadir, Y., Tromberg, B. J., and Berns, M. W. (1996). Dosimetry model for photodynamic therapy with topically administered photosensitizers. *Lasers in Surgery and Medicine*, 18(2):139–149.

Valentine, R., Brown, C., Moseley, H., Ibbotson, S., and Wood, K. (2011). Monte carlo modeling of in vivo protoporphyrin ix fluorescence and singlet oxygen production during photodynamic therapy for patients presenting with superficial basal cell carcinomas. *Journal of Biomedical Optics*, 16(4):048002–048002–11.

van den Akker, J. T. H. M., Iani, V., Star, W. M., Sterenborg, H. J. C. M., and Moan, J. (2000). Topical application of 5-aminolevulinic acid hexyl ester and 5-aminolevulinic acid to normal nude mouse skin: Differences in protoporphyrin ix fluorescence kinetics and the role of the stratum corneum. *Photochemistry and Photobiology*, 72(5):681–689.

Van Gemert, M., Jacques, S., Sterenborg, H., and Star, W. M. (1989). Skin optics. *Biomedical Engineering, IEEE Transactions on*, 36(12):1146–1154.

Wachowska, M., Muchowicz, A., Firczuk, M., Gabrysiak, M., Winiarska, M., Wanczyk, M., Bojarczuk, K., and Golab, J. (2011). Aminolevulinic acid (ala) as a prodrug in photodynamic therapy of cancer. *Molecules*, 16(5):4140–4164.

Wiegell, S., Hadersdal, M., Philipsen, P., Eriksen, P., Enk, C., and Wulf, H. (2008). Continuous activation of ppix by daylight is as effective as and less painful than conventional photodynamic therapy for actinic keratoses; a randomized, controlled, single-blinded study. *British Journal of Dermatology*, 158(4):740–746.

Wiegell, S., Heydenreich, J., Fabricius, S., and Wulf, H. (2011). Continuous ultra-low-intensity artificial daylight is not as effective as red led light in photodynamic therapy of multiple actinic keratoses. *Photodermatology, Photoimmunology Photomedicine*, 27(6):280–285.

Wiegell, S., Skodt, V., and Wulf, H. (2013). Daylight-mediated photodynamic therapy of basal cell carcinomas - an explorative study. *Journal of the European Academy of Dermatology and Venereology*.

Wiegell, S., Wulf, H., Szeimies, R.-M., Basset-Seguin, N., Bissonnette, R., Gerritsen, M.-J., Gilaberte, Y., Calzavara-Pinton, P., Morton, C., Sidoroff, A., and Braathen, L. (2012). Daylight photodynamic therapy for actinic keratosis: an international consensus. *Journal of the European Academy of Dermatology and Venereology*, 26(6):673–679.

Wilson, B. and Patterson, M. (2008). The physics, biophysics and technology of photodynamic therapy. *Physics in Medicine and Biology*, 53(9):R61.

Wood, K. (2013). http://www-star.st-and.ac.uk/ kw25/. *Monte Carlo Radiation Transfer*.

Wood, K. and R. J. Reynolds, R. (1999). A model for the scattered light contribution and polarization of the diffuse h galactic background. *The Astrophysical Journal*, 525(2):799.

Yudovsky, D. and Pilon, L. (2011). Retrieving skin properties from in vivo spectral reflectance measurements. *Journal of Biophotonics*, 4(5):305–314.